ELSEVIER

Biophysical Chemistry 118 (2005) 78 – 83

Biophysical Chemistry

http://www.elsevier.com/locate/biophyschem

A quantum chemical study on the mechanism of glycinamide ribonucleotide transformylase inhibitor: 10-Formyl-5,8,10-trideazafolic acid

Qing-An Qiao [a,*], Yueqing Jin [b], Chuanlu Yang [c], Zhihong Zhang [c], Meishan Wang [c]

[a] *School of Chemistry and Materials Science, Yantai Normal University, Yantai 264025, China*
[b] *Library of Yantai Normal University, Yantai 264025, China*
[c] *Department of Physics, Yantai Normal University, Yantai 264025, China*

Received 22 May 2005; received in revised form 1 July 2005; accepted 1 July 2005
Available online 28 September 2005

Abstract

A density functional theory (DFT) study is presented on the reaction mechanism of glycinamide ribonucleotide (GAR) with 10-formyl-5,8,10-trideazafolic acid (10f-TDAF), which is an inhibitor designed for GAR transformylase (GAR Tfase). There are three different paths for this system and the results indicate that inhibitor 10f-TDAF can form a very stable intermediate with the substrate GAR or generate an imine bond with GAR by elimination of water. The results have verified the presumption from available experiments and implied that 10f-TDAF would be an important target for anti-neoplastic intervention.

Keywords: GAR Tfase inhibitor; 10-Formyl-5,8,10-trideazafolic acid; Density Functional Theory (DFT)

1. Introduction

Glycinamide ribonucleotide transformylase (GAR Tfase, EC 2.1.2.2) is one of the two enzymes in the de novo purine biosynthetic pathway [1,2] that use 10-formyl-5,6,7,8-tetrahydrofolic acid (10f-THF) as a cofactor for formyl group transfer. It catalyzes the conversion of β-glycinamide ribonucleotide (GAR) to formyl-β-glycinamide ribonucleotide (f-GAR) (Fig. 1). Because of its association with purine nucleotides that are essential for many cellular processes, this enzyme has become the target of anti-neoplastic agents, in particular for cancer chemotherapy since rapidly dividing cells require large amount of purine [3–5]. More recently, a number of antifolates specific to GAR Tfase have been identified [6–11]. Habeck et al. [6] described the development of two promising selective GAR Tfase inhibitors based on the folate backbone. Boritzki et al. [7] described the synthesis and characterization of the inhibitor named AG2034. These inhibitors show specific, low nanomolar inhibition of GAR Tfase and in vivo antitumor activity and are presently being evaluated for potential clinical use. Boger et al. [12] and Greasley et al. [13] have reported the synthesis and characterization of 10-formyl-5,8,10-trideazafolic acid (10f-TDAF) (Fig. 1), a tetrahydrofolate analogue, which demonstrated simple competitive inhibition of GAR Tfase and did not exhibit tight binding or time-dependent inhibition. One possible explanation is that a rapid imine bond may be formed between 10f-TDAF and GAR [13]. Most recently, we have studied the catalytic mechanism of 10f-THF with GAR by means of density functional theory (DFT) [14] and a full examination on the mechanism of inhibitor 10f-TDAF and the comparison between the cofactor (10f-THF) and 10f-TDAF will be available this time. In the following calculations, only the GAR molecule and 10f-TDAF molecule are included as in Ref. [14]. Also,

* Corresponding author. Tel.: +86 535 6672176; fax: +86 535 6672574.
E-mail addresses: qiaoqa@sdu.edu.cn, qiaoqa@hotmail.com (Q.-A. Qiao).

0301-4622/$ - see front matter © 2005 Elsevier B.V. All rights reserved.
doi:10.1016/j.bpc.2005.07.001

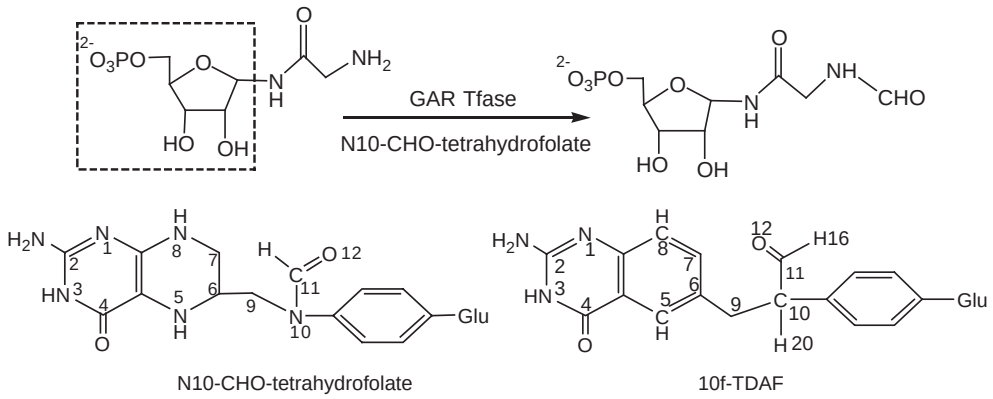

Fig. 1. The GAR Tfase catalyzed reaction and the molecular structures of 10f-THF and 10f-TDAF.

the ribonucleotide part of GAR molecule (cycled by the dashed line rectangle in Fig. 1) and the glutamic acid residue (Glu) in 10f-TDAF are replaced with hydrogen atoms as in Ref. [15].

2. Methodology

The full catalytic mechanisms of this model system are examined by the hybrid density functional theory (DFT) B3LYP [16] as implemented in the Gaussian03 program package [17], which method has previously been successfully applied to study a number of enzyme mechanisms [18]. The inherent accuracy of the B3LYP method can be estimated from benchmark tests [19], in which the average error in the atomization energies of the G2 set, consisting of 55 small first- and second-row molecules, is found to be 2.2 kcal/mol. When the 6-31G* and 6-311+G (3df, 2p) basis sets were used, the B3LYP hybrid functional was much preferred to the Hartree–Fock (HF) and MP2 methods. The average deviation for bond lengths is less than 0.02 Å and for angles and dihedrals less than 1°. Of course, the DFT method is not perfect and fails in treatment of dispersion-rich interactions, but it is successfully applied on many biological systems [20,21].

The structures of all reactants, intermediates, transition states and products are fully optimized at B3LYP/ 6-31G* level of theory. The most stable conformations as well as their energies at every equilibration and transition state have been figured out. Frequency calculations have been performed to all stationary points. The transition states have been identified by analyzing their vibrational modes and each has only one imaginary frequency.

3. Results and discussion

In the model system, 10f-TDAF (labelled as *b* in Fig. 2) can react with the substrate via three possible mechanisms: In principle, molecule *b* can react with GAR (referred as *a* in Fig. 2) to achieve the one-carbon unit transfer progress via *path a*, the concerted mechanism, as well as *path b*, the stepwise pathway. In addition, the reactants can experience a third way noted as *path c*, including an elimination of water and the formation of an imine bond.

3.1. Path a

In the concerted *path a*, *tsc* is the only transition state to connect the reactants and products. The bond length of C10–C11 has been elongated from an equilibrium value of 1.527 to 2.241 Å and considered nearly to break. With nucleophilic attack by N15, C11 begins to show some characters of sp3 hybridization. At the same time, the double bond of C11–O12 is stretched, increasing its single-bond character. The distance between N15 and C11 is 1.543Å, which is much closer to the normal length of a C–N single bond. The two reactants have their orbits overlapped with each other through a weak covalent bond. From Table 1, one can easily find out that the H17, C10, N15 and C11 atoms have formed a four-membered ring in *tsc*'s structure. The rupture of this ring will lead to the products, *g* and *h*. The dihedral of H17C10C11N15 is nearly zero suggesting a coplanar character of the ring, and the small angle of less than 90° for C11N15H17 and C10C11N15 shows strong strain in this system. The only imaginary frequency of *tsc* is 979.6i cm^{-1} and the normal vibrational modes analysis showed that H17 is the most reactive atom in this structure. The energy barrier for *tsc* is as high as 247.6 kJ/mol (Fig. 3), which is 15.2% higher than the activation energy of the transition state when the cofactor 10f-THF itself reacts with GAR via concerted mechanism [14]. The calculations for this pathway indicate that the 10f-TDAF molecule in the reactive centre can lead to a very high activation energy, which will make it very hard to transfer the –CHO group.

3.2. Path b

Transition state *tsd* is produced in the first migration of proton H17 from N15 to O12. There are four groups linked to N13 now and the system becomes unstable. As well as

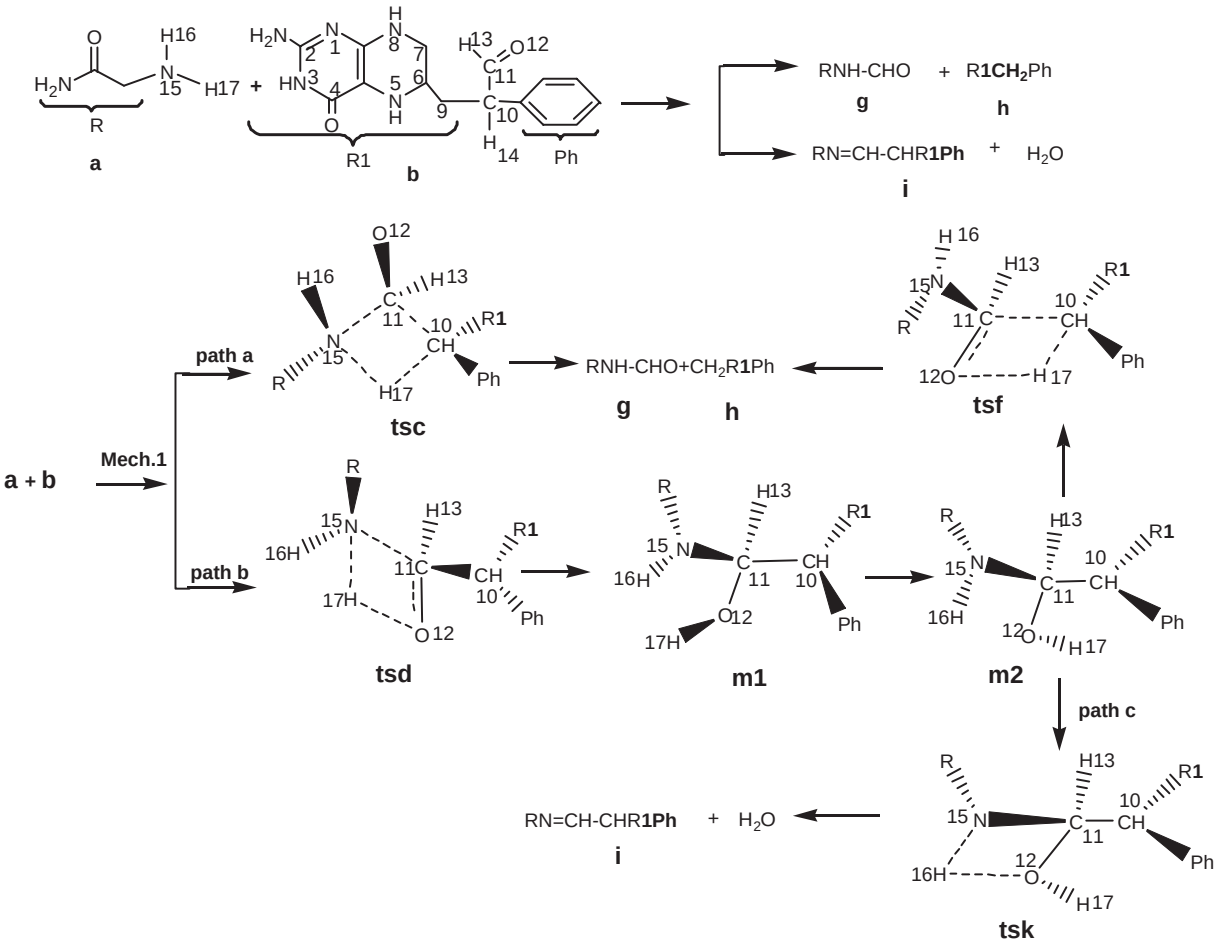

Fig. 2. The detailed reaction mechanism of 10f-TDAF and GAR.

tsc, there is a four-membered ring in *tsd*'s structure composed of the C11, N15, H17 and O12 atoms. As O12 is attacked by H17, the bond length of C11–O12 is getting longer, increasing its single bond character. The natural population analysis (NPA) [22] for *tsd* shows a more negative charge on O12 (−0.846) than on N15 (−0.748), while the natural charge population on H17 is 0.492, and it is inclined to form a covalent bond with O12.

Intermediate *m1* is located after the first migration of H17. The double bond of C–O has converted to a single bond completely. The lower relative energy of *m1* indicate its stability and this intermediate may remain in the reactive centre and prohibit the further process as Ref. [13] proposed. The orientation change of H17 results in another intermediate *m2*. It is a conformational isomer of *m1* and both of them are local minima on the potential energy surface. The alteration is necessary for the second proton transfer. The structure of *m2* is much closer to the structure of transition state *tsf*. The formyl group has changed to a hydroxymethyl group in both intermediates.

tsf is the transition state for the second migration of H17 which connects *m2* with the products. Due to the removal of H17, the bond length of C11–O12 is getting shorter and tends to reform a double bond. At the same time, C11 is apart from C10 and inclined to return to its sp2 hybridization state. The bond length of C11–C10 is 2.252 Å suggesting a very weak covalence between them and the four-membered ring composed of C11, O12, H17 and C10 is easy to rupture. The dihedral of H13C11O12N15 is −162.9° suggesting the hydroxymethyl group will reform a formyl group soon. Because there are two rings around C10 (the pterin ring and the benzene ring), the steric hindrance is an important factor to the proton transfer. This is why the relative energy for *tsf* is higher than that of *tsd*.

When compared with the reaction of the cofactor 10f-THF itself with GAR via stepwise mechanism [14], we find that it is favorable for the inhibitor 10f-TDAF to generate a very stable intermediate *m1* with the substrate and terminate the one-carbon unit transfer reaction (Fig. 3). Otherwise, the second transfer process of H17 will experience a very high energy barrier, which will be a hindrance to the –CHO migration.

3.3. Path c

Actually, *path c* is more like a side reaction of *path b*. After the successful transfer of H17 to O12, H16 could also migrate from N15 to O12 via transition state *tsk*. The bond length of

Table 1
The main structure data of the stationary points together with their relative energies

	Reactants**	tsc	tsd	m1	m2	tsf	tsk	Products**
Relative energy* (kJ/mol)	0	247.6	99.2	−47.1	−26.6	199.2	175.6	
Bond length (Å)								
N15H17(H16)	1.009[b]	1.111	1.212	–	–	–	1.331	–
H17C10	–	1.753	–	–	–	1.734	–	1.016[h]
N15C11	–	1.543	1.585	1.448	1.423	1.308	1.352	1.361[g]
								1.271[i]
C10C11	1.527[a]	2.241	1.558	1.558	1.567	2.252	1.531	1.517[i]
H17(H16)O12	–	–	1.383	0.971	0.971	1.115	1.253	
C11O12	1.210[a]	1.203	1.348	1.430	1.439	1.295	1.844	1.216
Bond angle (°)								
C11N15H17		87.7	72.6	–	116.3	–	78.7	
C11C10(O12)H17		47.2	76.2	–	107.5	57.3	63.3	
C10C11N15		80.0	113.9	117.7	115.3	112.9	120.2	123.8[i]
Dihedral (°)								
H13C11O12C10(N15)		162.3	−102.8	−115.6	−117.1	−162.9	−117.9	
H17C10(O12)C11N15		3.3	3.3	−21.3	−178.3	−118.5	–	

*The energy sum of the reactants was taken as zero.
**The values in the two columns are from the separated calculation results of a, b, g, h and i, as the superscript of the value indicated.

C11–N15 has been shortened from its equilibrium length of 1.423 to 1.352 Å, which means a larger orbital overlap between them than before. At the same time, the distance between C11 and O12 changes to1.844 Å and indicates the imminent rupture of C11O12. The natural charge population on O12 is −0.864, which is very close to the normal value of water oxygen (−0.934). The complete rupture will lead to an imine bond between C11 and N15. As shown in Fig. 3, *tsk* is favored to *tsf* duo to the low energy. In other words, *path c* is the preferable pathway to inhibit the –CHO transfer progress. The inhibitor would form an imine bond with the substrate rather than give the formyl group to it. From the energy profile (Fig 3, in which *path a′* and *path b′* indicate the –CHO transfer paths in Ref. [14]), one can find that once the inhibitor has located at the active centre, the formyl group transfer is getting much harder to take place and a stable intermediate or an imine complex will easily generate.

4. Conclusions

The following conclusions can be drawn from our calculations for the model system:

1) The inhibitor 10-formyl-5,8,10-trideazafolic acid can react with the substrate via both concerted and stepwise mechanisms. All the transition states have a four-membered ring in their structures indicating great tension in the system. The hydrogen atom being transferred is the most active in the stepwise mechanism.

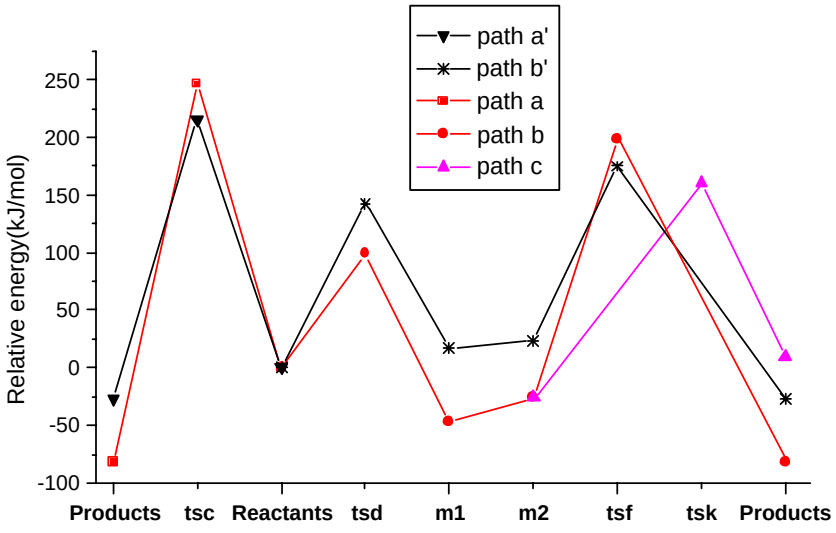

Fig. 3. The energy profiles of the reaction system compare to the –CHO transfer in Ref. [14].

2) Though the formyl group transfer might be achieved in principle, the inhibitor is much preferable to form a very stable intermediate (*path b*) or an imine complex by elimination of one water molecule (*path c*) due to the lower activation barrier.
3) The results from our calculations indicate that the presumption of Ref. [13] is quite conceivable and 10-formyl-5,8,10-trideazafolic acid would be an important target for anti-neoplastic intervention. It should be noticed that the effect of the residues (together with water molecules) in this reaction is out of consideration in the model system. In an actual system the whole reaction may be much easier to proceed due to the participation of enzyme and other medium, and the energy barriers may be lower than what we have calculated.

Acknowledgment

This work was supported by the Youth Natural Science Foundation of Yantai Normal University (No.042902), the Youth Natural Science Foundation of Shandong Provincial Education Department (No.200139) and the National Natural Scientific Foundation of China (No. 10404030 and No. 20373071).

References

[1] J. Aimi, H. Qiu, J. Williams, H. Zalkin, J.E. Dixon, De novo purine nucleotide biosynthesis: cloning of human and avian cDNAs encoding the trifunctional glycinamide ribonucleotide synthetase–aminoimidazole ribonucleotide synthetase–glycinamide ribonucleotide transformylase by functional complementation in *E. coli*, Nucleic Acids Res. 18 (1990) 6665–6672.
[2] P. Chen, U. Schulz-Gahmen, E.A. Stura, J. Inglese, D.L. Johnson, A. Marolewski, S.J. Benkovic, I.A. Wilson, Crystal structure of glycinamide ribonucleotide transformylase from *Escherichia coli* at 3.0 Å resolution, J. Mol. Biol. 227 (1992) 283–292.
[3] J.H. Shim, S.J. Benkovic, Catalytic mechanism of *Escherichia coli* glycinamide ribonucleotide transformylase probed by site-directed mutagenesis and pH-dependent studies, Biochemistry 38 (1999) 10024–10031.
[4] R.J. Almassy, C.A. Janson, C. Kan, Z. Hostomska, Structures of apo and complexed *Escherichia coli* glycinamide ribonucleotide transformylase, Proc. Natl. Acad. Sci. U. S. A. 89 (1992) 6114–6118.
[5] Y. Su, M.M. Yamashita, S.E. Greasley, C.A. Mullen, J.H. Shim, P.A. Jennings, S.J. Benkovic, I.A. Wilson, A pH-dependent stabilization of an active site loop observed from low and high pH crystal structures of mutant monomeric glycinamide ribonucleotide transformylase at 1.8 to 1.9 A, J. Mol. Biol. 281 (1998) 485–499.
[6] L.L. Habeck, T.A. Leitner, K.A. Shackelford, L.S. Gossett, R.M. Schultz, S.L. Andis, C. Shih, G.B. Grindey, L.G. Mendelsohn, A novel class of monoglutamated antifolatea exhibits tight-binding inhibition of human glycinamide ribonucleotide formyltransferase and potent activity against solid tumors, Cancer Res. 54 (1994) 1021–1026.
[7] T.J. Boritzki, C.A. Barlett, C. Zhang, E.F. Howland, S.A. Margosiak, C.L. Palmer, W.H. Romines, R.C. Jackson, AG2034: a novel inhibitor of glycinamide ribonucleotide formyltransferase, Invest. New Drugs 14 (1996) 295–303.
[8] C. Klein, P. Chen, J.H. Arevalo, E.A. Stura, A. Marolewski, M.S. Warren, S.J. Benkovic, I.A. Wilson, Towards structure-based drug design: crystal structure of a multisubstrate adduct complex of glycinamide ribonucleotide transformylase at 1.96 Å resolution, J. Mol. Biol. 249 (1) (1995) 153–175.
[9] H.M. Faessel, H.K. Slocum, R.C. Jackson, T.J. Boritzki, Y.M. Rustum, M.G. Nair, W.R. Greco, Super in vitro synergy between inhibitors of dihydrofolate reductase and inhibitors of other folate-requiring enzymes: the critical role of polyglutamylation, Cancer Res. 58 (1998) 3036–3050.
[10] Y. Zhang, J. Desharnais, T.H. Marsilje, C. Li, M.P. Hedrick, L.T. Gooljarsingh, A. Tavassoli, S.J. Benkovic, Ar.J. Olson, D.L. Boger, I.A. Wilson, Rational design, synthesis, evaluation, and crystal structure of a potent inhibitor of human GAR Tfase: 10-(trifluoroacetyl)-5,10-dideazaacyclic-5,6,7,8-tetrahydrofolic acid, Biochemestry 42 (2003) 6043–6056.
[11] J. Desharnais, I. Hwang, Y. Zhang, A. Tavassoli, J. Baboval, S.J. Benkovic, I. Wilson, D.L. Boger, Design, synthesis and biological evaluation of 10-CF3CO-DDACTHF analogues and derivatives as inhibitors of GARTfase and the de novo purine biosynthetic pathway, Bioorganic Med. Chem. 11 (2003) 4511–4521.
[12] D.L. Boger, N.E. Haynes, P.A. Kitos, M.S. Warren, J. Ramcharan, A.E. Marolewski, S.J. Benkovic, 10-Formyl-5,8,10-trideazafolic acid (10-formyl-TDAF): a potent inhibitor of glycinamide ribonucleotide transformylase, Bioorganic Med. Chem. 5 (1997) 1817–1830.
[13] S.E. Greasley, M.M. Yamashita, H. Cai, S.J. Benkovic, D.L. Boger, I.A. Wilson, New insights into inhibitor design from the crystal structure and NMR of *Escherichia coli* GAR transformylase in complex with β-GAR and 10-formyl-5,8,10-trideazafolic acid, Biochemistry 38 (1999) 16783–16793.
[14] Q.A. Qiao, Z.T. Cai, D.C. Feng, Y.S. Jiang, A quantum chemical study of the water-assisted mechanism in one-carbon unit transfer reaction catalyzed by glycinamide ribonucleotide transformylase, Biophys. Chem. 110 (2004) 259–266.
[15] Q.A. Qiao, Z.T. Cai, D.C. Feng, Quantum study on a new mechanism in one-carbon unit transfer reaction: the water-assisted mechanism, Chin. J. Chem. 22 (6) (2004) 505–507.
[16] C. Lee, W. Yang, R.G. Parr, Development of the Colle–Salvetti correlation-energy formula into a functional of the electron density, Phys. Rev., B 37 (1988) 785–789;
A.D. Becke, A new mixing of Hartree–Fock and local density-functional theories, J. Chem. Phys. 98 (1993) 1372–1377;
A.D. Becke, Density-functional thermochemistry: III. The role of exact exchange, J. Chem. Phys. 98 (1993) 5648–5652.
[17] Gaussian 03, Revision B.05, M.J. Frisch, G.W. Trucks, H.B. Schlegel, G.E. Scuseria, M.A. Robb, J.R. Cheeseman, J.A. Montgomery Jr., T. Vreven, K.N. Kudin, J.C. Burant, J.M. Millam, S.S. Iyengar, J. Tomasi, V. Barone, B. Mennucci, M. Cossi, G. Scalmani, N. Rega, G.A. Petersson, H. Nakatsuji, M. Hada, M. Ehara, K. Toyota, R. Fukuda, J. Hasegawa, M. Ishida, T. Nakajima, Y. Honda, O. Kitao, H. Nakai, M. Klene, X. Li, J.E. Knox, H.P. Hratchian, J.B. Cross, C. Adamo, J. Jaramillo, R. Gomperts, R.E. Stratmann, O. Yazyev, A.J. Austin, R. Cammi, C. Pomelli, J.W. Ochterski, P.Y. Ayala, K. Morokuma, G.A. Voth, P. Salvador, J.J. Dannenberg, V.G. Zakrzewski, S. Dapprich, A.D. Daniels, M.C. Strain, O. Farkas, D.K. Malick, A.D. Rabuck, K. Raghavachari, J.B. Foresman, J.V. Ortiz, Q. Cui, A.G. Baboul, S. Clifford, J. Cioslowski, B.B. Stefanov, G. Liu, A. Liashenko, P. Piskorz, I. Komaromi, R.L. Martin, D.J. Fox, T. Keith, M.A. Al-Laham, C.Y. Peng, A. Nanayakkara, M. Challacombe, P.M.W. Gill, B. Johnson, W. Chen, M.W. Wong, C. Gonzalez, J.A. Pople, Gaussian, Inc., Pittsburgh PA, 2003.
[18] P.E.M. Siegbahn, R.A.M. Blomberg, Transition-metal systems in biochemistry studied by high-accuracy quantum chemical methods, Chem. Rev. 100 (2000) 421–437 (and references therein).

[19] W. Charles Bauschlicher Jr., Comparison of the accuracy of different functionals, Chem. Phys. Lett. 246 (1995) 40–44;
C.W. Bauschlicher Jr., A. Ricca, H. Partridge, S.R. Langhoff, Recent Advances in Density Functional Methods, Part II, World Scientific Publishing Company, Singapore, 1997.

[20] A.F. Richard, Ab initio quantum chemistry: methodology and applications, Proc. Natl. Acad. Sci. U. S. A. 102 (10) (2005) 6648–6653.

[21] L.A. Curtiss, K. Raghavachari, P.C. Redfern, J.A. Pople, Assessment of Gaussian-3 and density functional theories for a larger experimental test set, J. Chem. Phys. 112 (2000) 7374–7383.

[22] J.E. Carpenter, F. Weinhold, Analysis of the geometry of the hydroxymethyl radical by the “different hybrids for different spins” natural bond orbital procedure, J. Mol. Struct., Theochem 169 (1988) 41–62.